Toward Cost-Effective Manufacturing of Silicon Solar Cells: Electrodeposition of High-Quality Si Films in a CaCl₂-based Molten Salt

Xiao Yang[+], Li Ji[+], Xingli Zou[+], Taeho Lim, Ji Zhao, Edward T. Yu, and Allen J. Bard*

Abstract: *Electrodeposition of Si films from a Si-containing electrolyte is a cost-effective approach for the manufacturing of solar cells. Proposals relying on fluoride-based molten salts have suffered from low product quality due to difficulties in impurity control. Here we demonstrate the successful electrodeposition of high-quality Si films from a CaCl₂-based molten salt. Soluble Si^{IV}–O anions generated from solid SiO₂ are electrodeposited onto a graphite substrate to form a dense film of crystalline Si. Impurities in the deposited Si film are controlled at low concentrations (both B and P are less than 1 ppm). In the photoelectrochemical measurements, the film shows p-type semiconductor character and large photocurrent. A p–n junction fabricated from the deposited Si film exhibits clear photovoltaic effects. This study represents the first step to the ultimate goal of developing a cost-effective manufacturing process for Si solar cells based on electrodeposition.*

Photovoltaic (PV) technologies for converting sunlight into electricity without toxic pollution or carbon emissions have received tremendous attention. Among the variety of materials that can serve as the major component of PV systems, silicon shows an outstanding advantage in technological reliability and natural availability. Cost is of primary importance in PV development. Solar-based electricity is expected to be cost-competitive in the United States at module costs of $ 0.50 to 0.75/Watt.[1] However, current manufacturing costs for Si solar modules are several times higher. Production of high-purity Si ingots by the Siemens process is highly energy-intensive, while slicing ingots to wafers (160 to 240 μm thick) by wire sawing results in considerable material loss in the form of kerf (width of each cut).[2] Therefore, in order to make solar-based electricity competitive, reducing the manufacturing costs for Si solar cells by means of a kerfless technology is desirable.

One promising approach is direct fabrication of Si films from inexpensive Si-based compounds via electrochemical techniques. Electrodeposition of crystalline Si films from fluoride-based molten salts has been investigated since the 1970s. Cohen first reported successful plating of Si films onto an Ag coated Si wafer in molten LiF–KF–K₂SiF₆.[3] Elwell et al.[4] and Bouteillon et al.[5] later obtained compact and smooth Si films on Ag or graphite substrates in molten LiF–NaF–KF–K₂SiF₆. Recently Yasuda et al. achieved relatively good quality deposits in molten KF–KCl, using K₂SiF₆ or SiCl₄ as the Si precursor.[6] Similar work or reviews can be found in the literature.[7] However, due to the difficulty in impurity control caused by the corrosive nature of fluorides, the obtained Si films exhibited no PV effects, and thus these techniques are yet pending for practical use. Therefore, a fluoride-free electrolyte is desirable to obtain high purity products with PV effects.

Molten CaCl₂ has attracted a lot of attention[8] since the work by Chen et al. on electro-deoxidation of solid TiO₂ to produce Ti metal.[9] Molten CaCl₂ offers several technical advantages as a high temperature electrolyte over fluorides: comparable high solubility of O²⁻ ions,[10] less corrosive nature,[11] and high solubility in water.[12] Nohira et al. systematically investigated the electrochemical reduction behaviors of solid SiO₂ in molten CaCl₂ and proposed a new production process for solar Si feedstock.[13] However, few reports on electrodeposition of high quality and photoactive Si films in CaCl₂-based molten salts can be found in the literature.[14]

Here, we demonstrate the successful deposition of dense Si films with high purity onto graphite from molten CaCl₂–CaO–SiO₂ at 1123 K. The film exhibits good photoelectrochemical properties and clear PV effects. We believe that this study has laid the foundation for a new process to manufacture Si solar cells via molten salt electrochemical techniques.

Previously, we had deposited photoactive Si films (about 4 μm thick) onto a silver or graphite substrate by using CaCl₂ as the electrolyte and SiO₂ nanoparticles (NPs) as the Si precursor.[15] However, fabrication of p–n junction with these films was impossible, because the small film thickness and high surface roughness that could be obtained precluded post processing. SiO₂ NPs suffer from low solubility in molten CaCl₂, limiting the net mass transport. Forming soluble ions from SiO₂ in molten CaCl₂ is considered to facilitate a high quality product. Packter et al. once studied the solubility of silicates in molten CaCl₂.[16] Stemmermann et al. studied the dissolution behavior of SiO₂ in molten CaCl₂–CaO.[17] Recently, electrodeposition of Si powder from soluble ions in CaCl₂-based molten salts were reported by several

[*] Dr. X. Yang,[+] Dr. L. Ji,[+] Dr. X. Zou,[+] Dr. T. Lim, Dr. J. Zhao,
    Prof. A. J. Bard
    Center for Electrochemistry, Department of Chemistry
    The University of Texas at Austin
    Austin, TX 78712 (USA)
    E-mail: ajbard@mail.utexas.edu

    Dr. L. Ji,[+] Prof. E. T. Yu
    Microelectronics Research Center, Department of Electrical and
    Computer Engineering, The University of Texas at Austin
    Austin, TX 78758 (USA)

[+] These authors contributed equally to this work.

groups.[18] Accordingly, we added CaO into $CaCl_2$ to optimize the electrolyte composition in the present study.

The role of CaO to favor Si electrodeposition was confirmed by cyclic voltammetry (CV) and potentiostatic electrolysis. Cyclic voltammogram of a Mo wire electrode is generally flat in pure $CaCl_2$ (dotted curve) contained in a SiO_2 crucible (Figure 1 a). After adding 1 mol% of CaO (solid
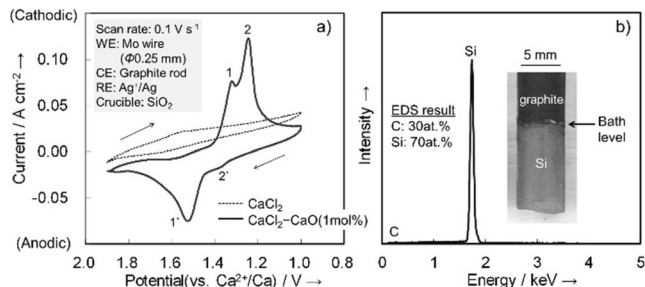

Figure 1. a) Cyclic voltammograms of a Mo wire in molten $CaCl_2$ and $CaCl_2$–CaO(1 mol%) in a SiO_2 crucible at 1123 K and b) a photograph of a graphite plate cathode after potentiostatic electrolysis at 0.7 V (vs. Ca^{2+}/Ca) for 10 min in molten $CaCl_2$–CaO(1 mol%) in a SiO_2 crucible at 1123 K and the EDS spectrum of the product on the surface.

curve), cathodic waves 1, 2 near 1.3 V (vs. Ca^{2+}/Ca) and anodic waves 1′, 2′ near 1.5 V appear clearly. CVs conducted in a larger potential range (Figure S3 in the Supporting Information) indicate the same tendency. EDS analysis of the product on a graphite plate cathode after potentiostatic electrolysis at 0.7 V (vs. Ca^{2+}/Ca) for 10 min in molten $CaCl_2$–CaO(1 mol%) confirms formation of Si on the cathode surface (Figure 1 b). It is proposed that O^{2-} ions dissociated from CaO react with the SiO_2 crucible to generate soluble Si^{IV}–O complex anions. Therefore, we can attribute waves 1 and 2 to deposition of Si from Si^{IV}–O anions, and waves 1′, 2′ to re-oxidation of Si. However, formation mechanism and electrochemical behavior of Si^{IV}–O anions in molten $CaCl_2$ are not well understood.

We tried to electrodeposit Si films onto graphite in molten $CaCl_2$ with addition of different amounts of CaO. SiO_2 NPs were used as the Si precursor to favor a fast dissolution. According to the product quality, we find that $CaCl_2$ with addition of 4.8 mol% of CaO and 3.9 mol% of SiO_2 NPs is the optimum composition. Excess CaO induces formation of Ca metal while excess SiO_2 NPs causes difficulty in complete dissolution in a short time. SiO_2 NPs suspended in the melt tend to form Si powders on cathode via direct electrochemical reduction (Figure S4).[13a]

By optimizing the electrolyte composition, we made significant progress in film thickness and quality compared with our previous work.[15] Dense crystalline Si films (thickness up to 35 μm) were deposited onto a graphite substrate by constant current electrolysis in the two-electrode manner (Figures 2 and S5). The current of 15 mA cm^{-2} is considered an optimum value (Figure S6). Formation mechanism is proposed in Figure 3. In the molten salt, solid SiO_2 NPs react with O^{2-} to form soluble Si^{IV}–O anions, which are reduced to Si atoms on the graphite surface by obtaining
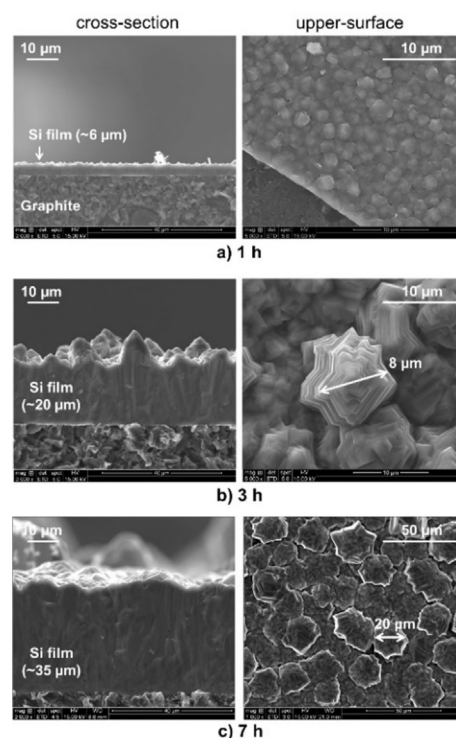

Figure 2. SEM images of the Si films deposited on graphite substrates in molten $CaCl_2$–CaO–SiO_2 (CaO: 4.8 mol%, SiO_2: 3.9 mol%) at 1123 K by electrolysis at a constant cathodic current of 15 mA cm^{-2} for a) 1 h, b) 3 h and c) 7 h.
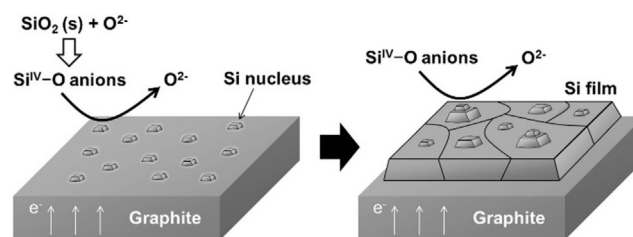

Figure 3. Formation mechanism of Si film onto a graphite substrate by electrodeposition in molten $CaCl_2$–CaO–SiO_2.

electrons. A uniform Si film is gradually formed after nucleation and crystallization. O^{2-} isolated from Si^{IV}–O anions diffuse toward the graphite anode and leave the system as CO or CO_2. Increase of film thickness and grain size indicates the continuous progress of electrodeposition and crystallization. Current efficiency is about 40% to form the 20 μm film (Figure S7). However, the film formation efficiency decreases with electrolysis time. Accumulation of powders on film surface during electrolysis is the reason for the decreasing efficiency. We believe that generating soluble Si^{IV}–O anions to a certain concentration while getting rid of suspended SiO_2 particles in molten salt are the keys to produce a good film.

Chemical composition of a deposited Si film was analyzed by glowing discharge mass spectrometry (GDMS). The result (Table 1) indicates low impurity concentrations. B and P, both regarded as the most problematic elements for solar Si, are

Table 1: Chemical composition of a Si film deposited at a constant cathodic current of 15 mA cm^{-2} for 3 h in molten CaCl$_2$–CaO–SiO$_2$ (CaO: 4.8 mol%, SiO$_2$: 3.9 mol%) at 1123 K, analyzed by GDMS.

Element[a]	Concentration[b]	Element	Concentration
B	0.9	Ca	250
F	<5	Ti	0.9
Na	6.9	Mn	0.7
Mg	5.7	Fe	<0.5
Al	10	Cu	4.8
P	0.6	Br	3.2
S	2	Zr	2.2
Cl	330	W	13

[a] C, H, and O are not determined; impurities less than 0.5 ppm are not listed. [b] Unit: ppm by weight.

0.9 ppm and 0.6 ppm, respectively. Other impurities except Ca and Cl are all less than 10 ppm. We consider that residual CaCl$_2$ on the film surface due to insufficient rinsing is the major source of Ca and Cl. However, thermodynamic data (Figure S8) implies that decomposition of CaO is possible during electrolysis to form dilute Ca–Si alloys because of the small activity of Ca in Si.[19] We will investigate the alloys formation by checking the chemical state of Ca in the future study. Na, Mg and Al may come from CaCl$_2$. W is from the electrode material. Other impurities may also derive from CaCl$_2$ or the SiO$_2$ crucible. We believe that there is large room for further improvement by using high-purity raw materials and optimizing the operation. Our progress indicates good prospects of high-purity Si production via electrochemical techniques using CaCl$_2$-based molten salts.

In photoelectrochemical measurements, the deposited Si films exhibit a p-type semiconductor character: shift of open circuit potentials to more positive values under illumination due to movement of the positively charged holes away from the surface toward the Si bulk (Figure 4a). Because of flowing of excited electrons in the conduction band across the semiconductor/solution interface, ethyl viologen cations (EV^{2+}) in the solution are reduced into EV$^+$, and cathodic photocurrent is induced (Figure 4b). According to the impurity concentrations (Table 1), we consider that Al having three valence electrons is most likely the dominant p-type dopant for the deposited Si films. Doping proceeds electrochemically during electrodeposition. However, the doping mechanism is not well understood.

Shift of open circuit potential by illumination from darkness for the 20 μm film (about 0.25 V) is larger compared with that of the 7 μm film (about 0.11 V), indicating the difference in the amount of excited electrons. Larger film thickness and higher film quality result in better photoelectrochemical properties. In the case of the thinner film (7 μm), photocurrent is 1.1 mA cm^{-2} at −0.62 V (vs. Ag/AgNO$_3$). Dark current originating from the exposed graphite surface increases at more negative potentials, indicating many undesired pinholes or cracks in the film. For the thicker film (20 μm), photocurrent reaches 3.3 mA cm^{-2} at −0.62 V (vs. Ag/AgNO$_3$), amounting to 36% that of the commercial p-type Si wafer (about 9.1 mA cm^{-2}), while dark current is relatively small even at more negative potentials. According to replicated measurements on the same sample, we found
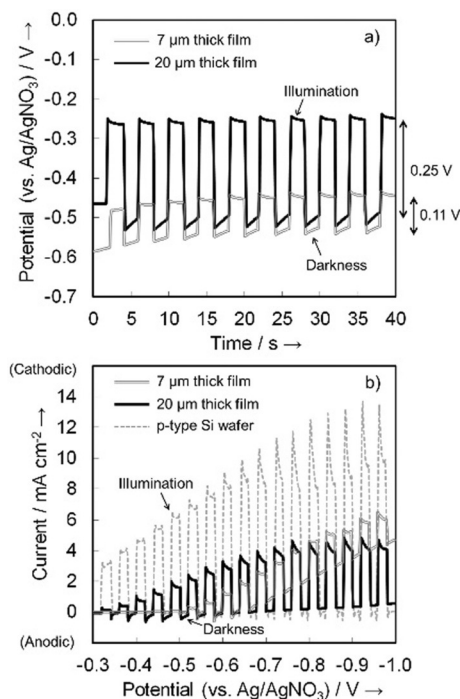

Figure 4. a) Variation of open circuit potentials for the deposited Si films and b) photocurrent–potential characteristics for the deposited Si films and a p-type Si wafer in darkness and under illumination at 100 mW cm^{-2}. Light was chopped at an interval of 2 s.

good stability of the photoelectrochemical properties of the deposited film. Large photocurrent implies the high purity of the deposited Si films, although still not as large as the commercial wafer.

Due to the improved film quality, a p–n junction was successfully fabricated by using the 20 μm Si film (Figure S2). As indicated by current–voltage characteristics (Figure 5), the junction exhibits good diode rectifying behaviour in darkness (dotted curve) and clear PV effects under illumination (solid curve). When illuminated, open circuit potential (V_{oc}) is 52 mV, short circuit current (J_{sc}) is 3.3 mA cm^{-2}, and power conversion efficiency (PCE) is estimated to be about 0.1%.
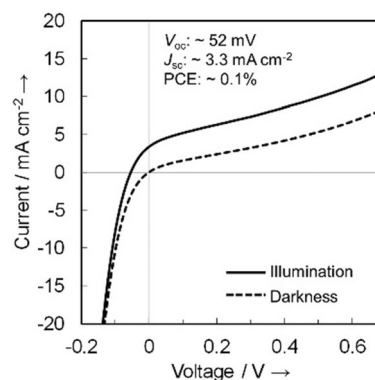

Figure 5. Current–voltage characteristics of a p–n junction fabricated from the deposited Si film in darkness and under illumination (AM1.5G, 100 mW cm^{-2}).

To the best of our knowledge, this is the first report on electrodeposition of Si films exhibiting clear PV effects. Optimization of parameters and implementation of post-treatments are likely to improve the film quality to approach or satisfy the requirements of a commercial application. Accordingly, we propose a new process via molten salt electrodeposition to manufacture Si solar cells. Multiple steps (primary reduction and downstream casting and slicing, doping) in the conventional process are integrated into one step (electrodeposition) in the new process (Figure 6).
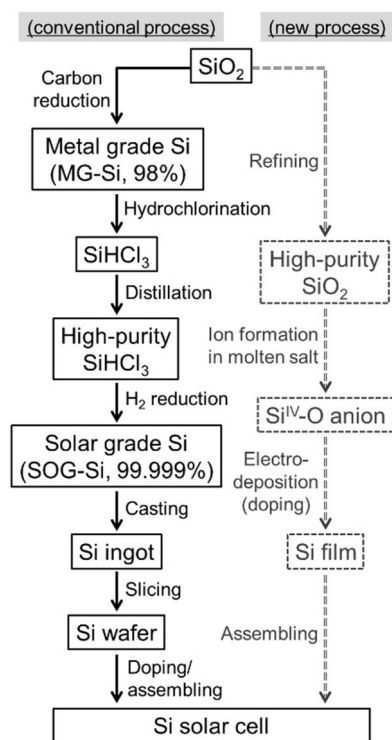

Figure 6. A comparison between the proposed new process via molten salt electrodeposition and the conventional process via carbon reduction to manufacture Si solar cells.

Dopant type and concentration could be controlled by adjusting additive type and quantity in molten salt. Therefore, a considerable cost reduction with the new process would be expected. The process could be further simplified by formation of the p–n junction electrochemically, which is currently being investigated.

In conclusion, we have shown a successful electrodeposition of high-quality Si films in molten $CaCl_2$–CaO–SiO_2 at 1123 K. Soluble Si^{IV}–O anions are generated and electrodeposited onto a graphite substrate to form a dense and thick Si film. We find that $CaCl_2$ with addition of 4.8 mol% of CaO and 3.9 mol% of SiO_2 NPs is the optimum composition. The electrodeposited Si films have the following properties: 1) dense and compact; 2) thickness up to 35 μm; 3) low impurity concentrations; 4) p-type semiconductor character with Al as the dominant dopant; 5) good photoelectrochemical properties and clear PV effects. This study represents the first step to develop a cost-effective manufacturing process for Si solar cells via molten salt electrochemical techniques.

Conflict of interest

The authors declare no conflict of interest.

[1] D. M. Powell, M. T. Winkler, H. Choi, C. B. Simmons, D. B. Needleman, T. Buonassisi, *Energy Environ. Sci.* **2012**, *5*, 5874–5883.

[2] a) T. Saga, *NPG Asia Mater.* **2010**, *2*, 96–102; b) G. Bye, B. Ceccaroli, *Sol. Energy Mater. Sol. Cells* **2014**, *130*, 634–646.

[3] a) U. Cohen, R. A. Huggins, *J. Electrochem. Soc.* **1976**, *123*, 381–383; b) U. Cohen, *J. Electron. Mater.* **1977**, *6*, 607–643.

[4] a) G. M. Rao, D. Elwell, R. S. Feigelson, *J. Electrochem. Soc.* **1980**, *127*, 1940–1944; b) G. M. Rao, D. Elwell, R. S. Feigelson, *J. Electrochem. Soc.* **1981**, *128*, 1708–1711; c) D. Elwell, G. Rao, *Electrochim. Acta* **1982**, *27*, 673–676; d) D. Elwell, G. M. Rao, *J. Appl. Electrochem.* **1988**, *18*, 15–22.

[5] a) R. Boen, J. Bouteillon, *J. Appl. Electrochem.* **1983**, *13*, 277–288; b) J. De Lepinay, J. Bouteillon, S. Traore, D. Renaud, M. Barbier, *J. Appl. Electrochem.* **1987**, *17*, 294–302.

[6] a) K. Maeda, K. Yasuda, T. Nohira, R. Hagiwara, T. Homma, *J. Electrochem. Soc.* **2015**, *162*, D444–D448; b) K. Yasuda, K. Maeda, T. Nohira, R. Hagiwara, T. Homma, *J. Electrochem. Soc.* **2016**, *163*, D95–D99; c) K. Yasuda, K. Maeda, R. Hagiwara, T. Homma, T. Nohira, *J. Electrochem. Soc.* **2017**, *164*, D67–D71.

[7] a) K. Carleton, J. Olson, A. Kibbler, *J. Electrochem. Soc.* **1983**, *130*, 782–786; b) K. S. Osen, A. M. Martinez, S. Rolseth, H. Gudbrandsen, M. Juel, G. M. Haarberg, *ECS Trans.* **2010**, *33*, 429–438; c) A. L. Bieber, L. Massot, M. Gibilaro, L. Cassayre, P. Taxil, P. Chamelot, *Electrochim. Acta* **2012**, *62*, 282–289; d) G. M. Haarberg, L. Famiyeh, A. M. Martinez, K. S. Osen, *Electrochim. Acta* **2013**, *100*, 226–228; e) J. Xu, G. M. Haarberg, *High Temp. Mater. Processes* **2013**, *32*, 97–105; f) Y. Sakanaka, T. Goto, *Electrochim. Acta* **2015**, *164*, 139–142; g) S. I. Zhuk, A. V. Isakov, A. P. Apisarov, O. V. Grishenkova, V. A. Isaev, E. G. Vovkotrub, Y. P. Zaykov, *J. Electrochem. Soc.* **2017**, *164*, H5135–H5138.

[8] a) X. Jin, P. Gao, D. Wang, X. Hu, G. Z. Chen, *Angew. Chem. Int. Ed.* **2004**, *43*, 733–736; *Angew. Chem.* **2004**, *116*, 751–754; b) K. Jiang, X. Hu, M. Ma, D. Wang, G. Qiu, X. Jin, G. Z. Chen, *Angew. Chem. Int. Ed.* **2006**, *45*, 428–432; *Angew. Chem.* **2006**, *118*, 442–446; c) D. Wang, G. Qiu, X. Jin, X. Hu, G. Z. Chen, *Angew. Chem. Int. Ed.* **2006**, *45*, 2384–2388; *Angew. Chem.* **2006**, *118*, 2444–2448; d) D. Hyslop, A. Abdelkader, A. Cox, D.

Fray, *Acta Mater.* **2010**, *58*, 3124–3130; e) W. Xiao, D. Wang, *Chem. Soc. Rev.* **2014**, *43*, 3215–3228.

[9] G. Z. Chen, D. J. Fray, T. W. Farthing, *Nature* **2000**, *407*, 361–364.

[10] D. A. Wenz, I. Johnson, R. D. Wolson, *J. Chem. Eng. Data* **1969**, *14*, 250–252.

[11] G. J. Janz, R. P. Tomkins, *Corrosion* **1979**, *35*, 485–504.

[12] A. Seidell, *Solubilities of Inorganic and Organic Compounds: A Compilation of Quantitative Solubility Data From the Periodical Literature*, D. Van Nostrand Company, New York, **1919**, p. 196.

[13] a) T. Nohira, K. Yasuda, Y. Ito, *Nat. Mater.* **2003**, *2*, 397–401; b) T. Toba, K. Yasuda, T. Nohira, X. Yang, R. Hagiwara, K. Ichitsubo, K. Masuda, T. Homma, *Electrochemistry* **2013**, *81*, 559–565; c) X. Yang, K. Yasuda, T. Nohira, R. Hagiwara, T. Homma, *Metall. Mater. Trans. B* **2014**, *45*, 1337–1344; d) X. Yang, K. Yasuda, T. Nohira, R. Hagiwara, T. Homma, *J. Electrochem. Soc.* **2014**, *161*, D3116–D3119; e) X. Yang, K. Yasuda, T. Nohira, R. Hagiwara, T. Homma, *Metall. Mater. Trans. B* **2016**, *47*, 788–797; f) X. Yang, K. Yasuda, T. Nohira, R. Hagiwara, T. Homma, *Metall. Mater. Trans. E* **2016**, *3*, 145–155.

[14] Y. Sakanaka, A. Murata, T. Goto, K. Hachiya, *J. Alloys Compd.* **2017**, *695*, 2131–2135.

[15] a) S. K. Cho, F. F. Fan, A. J. Bard, *Electrochim. Acta* **2012**, *65*, 57–63; b) S. K. Cho, F. F. Fan, A. J. Bard, *Angew. Chem. Int. Ed.* **2012**, *51*, 12740–12744; *Angew. Chem.* **2012**, *124*, 12912–12916; c) J. Zhao, H. Yin, T. Lim, H. Xie, H. Hsu, F. Forouzan, A. J. Bard, *J. Electrochem. Soc.* **2016**, *163*, D506–D514.

[16] A. Packter, S. Zaidi, *Z. Phys. Chem.* **1982**, *263*, 481–489.

[17] P. Stemmermann, H. Pöllmann, *N. Jb. Miner. Mh.* **1992**, *9*, 409–431.

[18] a) O. E. Kongstein, C. Wollan, S. Sultana, G. M. Haarberg, *ECS Trans.* **2007**, *35*, 357–361; b) J. Cai, X. Luo, G. M. Haarberg, O. E. Kongstein, S. Wang, *J. Electrochem. Soc.* **2012**, *159*, D155–D158; c) K. Yasuda, T. Nohira, R. Hagiwara, Y. H. Ogata, *J. Electrochem. Soc.* **2007**, *154*, E95–E101; d) W. Xiao, X. Wang, H. Yin, H. Zhu, X. Mao, D. Wang, *RSC Adv.* **2012**, *2*, 7588–7593.

[19] J. R. Wynnyckyj, L. M. Pidgeon, *Metall. Trans.* **1971**, *2*, 975–978.